Small Molecule Therapeutics

Molecular Cancer Therapeutics

Developing Lipid Nanoparticle-Based siRNA Therapeutics for Hepatocellular Carcinoma Using an Integrated Approach

Leiming Li[1], Rongqi Wang[1], Denise Wilcox[1], Aparna Sarthy[1], Xiaoyu Lin[1], Xiaoli Huang[1], Lu Tian[1], Prasad Dande[1], Robert D. Hubbard[1], Todd M. Hansen[1], Carol Wada[1], Xiaobin Zhao[2], William M. Kohlbrenner[1], Stephen W. Fesik[1], and Yu Shen[1]

Abstract

Successful siRNA therapeutics requires the optimal integration of multiple components, including an efficient delivery system, a disease indication that is appropriate for siRNA-based therapy, and a potent and nontoxic siRNA against a robust therapeutic target. Although all currently available delivery systems have limitations, it is important to recognize that a careful selection of the disease indication, therapeutic target, and siRNA molecule could partially compensate for deficiencies associated with the delivery system and makes it possible to advance a therapeutic siRNA regimen. In this study, we present the development of siRNA therapeutics for hepatocellular carcinoma using an integrated approach, including the development of an efficient lipid nanoparticle delivery system, the identification of a robust therapeutic target that does not trigger liver toxicity upon target knockdown, and the selection of potent and nonimmunogenic siRNA molecules against the target. The resulting siRNA-containing lipid nanoparticles produced significant antitumor efficacy in orthotopic hepatocellular carcinoma models, and, thus, represent a promising starting point for the development of siRNA therapeutics for hepatocellular carcinoma. *Mol Cancer Ther; 12(11); 2308–18. ©2013 AACR.*

Introduction

siRNA represents a promising novel therapeutic modality for the treatment of cancer (1). However, delivering siRNA to tumors using clinically acceptable delivery strategies remains a major technical hurdle (2, 3). Over the last 10 years, various proof-of-concept successes of *in vivo* siRNA delivery to tumors have been reported using delivery vehicles such as liposomes, cationic polymers, and other materials (4–10). To select the most promising delivery platform for the development of siRNA therapeutics, we evaluated the majority of available delivery technologies for their abilities to deliver siRNA into tumors using the previously described positive-readout tumor models (11). From these analyses, lipid nanoparticles such as stable nucleic acids lipid nanoparticles (SNALP) emerged as the most promising platform for tumor delivery via systemic administration. SNALP is a lipid nanoparticle of ~100 nm in size and has a close to neutral surface charge (10, 12, 13). It consists of cholesterol, DSPC, D-Lin-DMA and PEG-C-DMA. Among these components, the neutral lipids DSPC and cholesterol are commonly used in many liposome formulations for maintaining liposome structure whereas PEG-C-DMA and D-Lin-DMA are unique components of SNALP that are critical for its *in vivo* delivery efficiency (14, 15).

Although delivery is often the primary focus of most therapeutic siRNA programs, it is important to recognize that a successful siRNA drug requires an optimal integration of multiple components: an efficient delivery system, a potent nontoxic siRNA, a robust therapeutic target, and a carefully selected disease indication. Because all current delivery technologies have various limitations, a careful selection of the disease indication, disease target, and siRNA sequences will likely be required to compensate for deficiencies associated with current delivery technologies to maximize the chances of success.

Here we report the development of a siRNA-based approach for the treatment of hepatocellular carcinoma (HCC) using an integrated approach, including the discovery of a siRNA delivery system that has equivalent tumor delivery efficiency but reduced adverse effect compared with SNALP, and the identification of therapeutic targets and siRNA molecules that allow selective targeting of liver tumors without triggering overt liver toxicity. The resulted siRNA-containing lipid nanoparticles produced robust antitumor efficacy in an orthotopic HCC model, and thus, represents a promising starting point for the development of siRNA therapies for HCC.

Authors' Affiliations: [1]Cancer Research and [2]Global Pharmaceutical and Analytical Sciences, Abbott Laboratories, Abbott Park, Illinois

Corresponding Author: Yu Shen, Cancer Research, Global Pharmaceutical and Analytical Sciences, Abbott Laboratories, 100 Abbott Park Road, Abbott Park, IL 20064. Phone: 847-936-1128; Fax: 847-936-1128; E-mail: yu.shen@abbott.com

doi: 10.1158/1535-7163.MCT-12-0983-T

Materials and Methods

Reagents and cell lines

The positive readout reporter cell line, Tet-ODC-Luc, and the TetR siRNA used in the study were previously described (11). HepG2 and HuH7 cells were obtained from American Type Culture Collection more than 10 years ago. Aliquots of low-passage cells from original purchasing were kept in liquid nitrogen and were revived and cultured at conditions suggested by the vendor. The revived cells were passaged in culture for less than 3 months before replaced with a newly revived batch for experiments. D-Lin-DMA, PEG-C-DMA, and various proprietary cationic lipids and polyethylene glycol (PEG) lipids were synthesized at Abbott (16). The poly (I:C) was purchased from Sigma. Human RAN antibody was obtained from Cell Signaling.

Lipid nanoparticle formulation

SNALP was prepared according to the literature-described procedure (7). D-Lin-DMA and PEG-C-DMA were formulated with DSPC, cholesterol, and siRNA using a 25:1 lipid/siRNA ratio and a 48/40/10/2 molar ratio of cholesterol/D-Lin-DMA/DSPC/PEG-C-DMA. The resulted SNALP liposomes have similar characteristics to what was described in the literature (80–100 nm in size, PDI < 0.1, and a close to neutral ξ potential). Lipid nanoparticles containing in-house lipids were prepared using a needle injection method that was described earlier (17). Briefly, solutions of lipid mixtures were prepared in ethanol, injected into siRNA-containing citrate buffer through a 27-gauge needle. The resulted particle suspension was then diluted in PBS (pH 7.4) followed by 4 cycles of diafiltration against PBS, sterile filtered, and stored at 4°C.

Tumor models, animal dosing, and bioluminescence imaging analysis

The animal studies were carried out in accordance with internal Institutional Animal Care and Use Committee guidelines at Abbott Laboratories. All animals were obtained from Charles River Laboratory. TetR-ODC-Luc, HepG2, or HuH7 cells were inoculated into the liver of 6- to 8 week-old severe combined immunodeficient (SCID) female mice to create various liver tumor models. For *in vivo* knockdown evaluation in the positive-readout model, treatments were started 3 to 4 weeks after tumor inoculation for liver tumors. Mice bearing the TetR-ODC-Luc-derived liver tumors were imaged on day 1, administrated with lipid nanoparticles on day 1 and day 2 (i.v. 2.5 mg siRNA/kg), and reimaged on day 4 (48 hours after the last dose). *In vivo* bioluminescence imaging and analysis were conducted on the IVIS 200 system using the Living Image acquisition and analysis software (Caliper Life Science) as previously described (11). Briefly, after intraperitoneal injection of luciferin (Promega) at 150 mg/kg, mice were anesthetized with isofluorane. Four minutes after the injection of luciferin, a series of time-lapse images were acquired at 2 minutes intervals in a total of 10 minutes. Region of interest (ROI) were drawn around the tumors and signal intensity was quantified as the sum of photon counts per second within the ROI after the subtraction of background luminescence. The peak reading during the 10-minute imaging period was used for calculating the signal ratio before and after siRNA delivery. For antitumor efficacy studies, lipid nanoparticles were administered 72 hours after cancer cell inoculation (i.v. 2.5 mg siRNA/kg, twice/week for 3 weeks). At the end of the efficacy trial, mice were humanly euthanized, and liver tumor nodules were surgically excised and weighted. For mice without visible tumors, the tumor weight was recorded as 0.

Separate liposomes from liposome/serum mixture

Sepharose column was prepared by adding Sepharose CL-4B (Sigma) into 1.2 mL plastic column (Bio-Rad) followed by centrifugation at 1,000 rpm for 1 minute (Beckman ALGRA 6R). The Sepharose column was further washed once with 0.2 mL PBS. Freshly prepared column was loaded with 100 μL of liposome/FBS mixture and centrifuged at 1,000 rpm for 1 minute to collect the elute for MS analysis.

In vivo tolerability assessment

Lipid nanoparticles containing different siRNAs were administered to nontumor-bearing SCID females via intravenous injection at 2.5 mg siRNA/kg, twice/week, for 3 weeks. At the end of the study, mice were humanely euthanized, serum ALT and AST levels were determined, and liver morphology was examined. Lipid nanoparticles that triggered significant increase of ALT or AST levels (>4-fold over untreated control group), or >10% weight loss, or gross liver morphology changes (e.g., liver color change, liver fibrosis, etc.) were designated as intolerable.

Determination of siRNA-mediated immune response

Lipid nanoparticles containing different siRNAs were intravenously administered at 2.5 mg siRNA/kg. Serum samples were harvested 2 hours after dosing, and the levels of a panel of cytokines and chemokines were determined using a multiplex assay (Luminex).

Results

Impact of PEG shields on *in vitro* and *in vivo* activities of lipid nanoparticles

The PEG lipid engrafts on lipid nanoparticles to form a PEG shield that tends to limit particle clearance by the reticular endothelial system, and therefore, is an essential component for modulating the PK properties that are critical for *in vivo* delivery. To better understand the impact of PEG shielding on *in vitro* and *in vivo* activities of lipid nanoparticles, we created SNALP-like lipid nanoparticles that contain PEG molecules with C14 (PEG-DMPE), C16 (PEG-DPPE), and C18 (PEG-DSPE) lipid anchors. These lipid nanoparticles encapsulate a siRNA targeting tet repressor (siTetR), thus allowing convenient *in vitro* and *in vivo* testing using the previously described TetR-ODC-Luc cells, a positive-readout cell line where

successful delivery of siTetR into cells leads to an increase of luciferase activity (11). Incubating lipid nanoparticles containing PEG-DMPE with TetR-ODC-Luc resulted in a robust increase of luciferase reporter activity, indicating efficient delivery of the tetR siRNA into these cells. Lipid nanoparticles containing PEG-DPPE and PEG-DSPE only exhibited moderate and marginal activities, suggesting that these particles deliver siRNAs into cells less efficiently (Fig. 1A). Surprisingly, the *in vivo* activities of lipid nanoparticles containing different PEG lipids exhibited an opposite trend. Particles with PEG-DPPE and PEG-DPSE triggered an increase of luminescence in an orthotopic

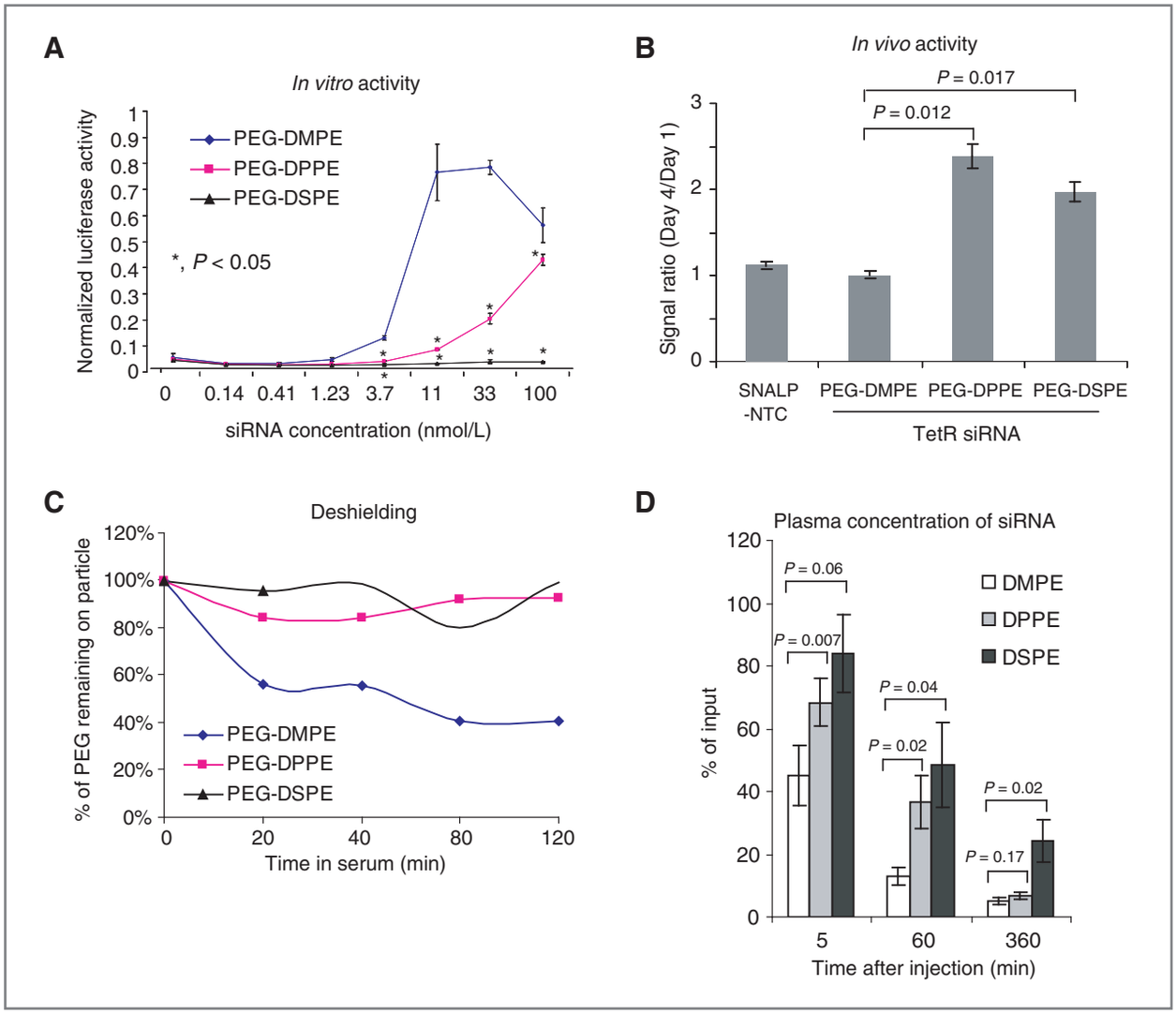

Figure 1. The impact of PEG lipids on *in vitro* and *in vivo* activities of lipid nanoparticles. A, different amounts of the SNALP-like lipid nanoparticles containing different PEG lipids and the TetR siRNA were incubated with the positive-readout cell line TetR-ODC-Luc for 72 hours. Luciferase activities were determined using the SteadyGlo Luciferase Assay kit. The resulting luciferase activities in lipid nanoparticle-treated cells were normalized to the luciferase activity in TetR-ODC-Luc cells treated with doxycycline for 3 days, and the normalized results were presented as normalized luciferase activity. *P* values for each dose were calculated by comparing to the PEG-DMPE group using paired 2 tail *t* test. B, SNALP containing a nontargeted control siRNA (SNALP-NTC) or SNALP-like nanoparticles containing different PEG lipids and the TetR siRNA were administered to mice bearing the TetRODC-Luc–derived liver tumors (i.v. 2.5 mg siRNA/kg for 2 consecutive days; $n = 5$/group). Mice were imaged before dosing (Day 1) and 48 hours after last dose (Day 4). Higher Day 4/Day 1 signal ratio indicates better knockdown of TetR in tumors after lipid nanoparticle-mediated siRNA delivery. *P* values were obtained by comparing the indicated treatment groups using paired 2 tail *t* test. C, SNALP-like lipid nanoparticles containing different PEG lipids and the TetR siRNA were incubated with FBS for indicated time. Intact lipid nanoparticles were then recovered using a sepharose spin column and the amounts of each PEG lipid on particle were determined using LC-MS. *Y*-axis represents the percentage of PEG lipid that remains on particle at each time point compared with the amount of PEG lipid in the original particle. D, siRNA-containing lipid nanoparticles with different PEG lipids were administered to nontumor-bearing mice ($n = 3$/group). The amount of lipid nanoparticle encapsulated siRNA in circulation at the indicated time was quantified and the value was used to back calculate the amounts of lipid nanoparticles remaining in circulation. The resulting amounts of circulating nanoparticles were further normalized to the total amount of nanoparticles administered to obtain the "% of input" number that is presented in the figure. *P* values were obtained by comparing the indicated treatment groups using paired 2 tail *t* test.

liver tumor model created using the TetR-ODC-Luc cells, indicating successful delivery of the TetR siRNA into tumors. In contrast, particles with PEG-DMPE seemed to be inactive *in vivo* (Fig. 1B).

PEG-lipids on liposome can interact with plasma proteins and be extracted/exchanged to plasma proteins, resulting in the deshielding of liposome. The deshielded "naked" liposomes will have vastly different pharmacokinetic properties compared to liposomes with PEG shields. We suspected that the PEG shield anchored by DMPE, DPPE, or DSPE may deshield differently and consequently affect the pharmacokinetics property and *in vivo* delivery efficiency of liposomes. To test this hypothesis, we examined the deshielding property of various lipid nanoparticles by incubating the lipid nanoparticles with serum, recovering intact particles overtime using Sepharose spin columns, and quantifying remaining PEG-lipid on the particle. As shown in Fig. 1C, PEG-DMPE quickly dissociated from lipid nanoparticle; whereas, no apparent deshielding was observed in the same time frame for PEG-DPPE and PEG-DSPE. Consistent with their rapid deshielding, the PEG-DMPE-containing particles quickly disappeared from systemic circulation after intravenous administration (a >50% reduction of circulating particles within 5 minutes and nearly 90% reduction of circulating particles at 60 minutes). In contrast, the PEG-DPPE- and PEG-DSPE-containing particles stayed in circulation for a much longer period of time (>70% particles remained in circulation at 5 minutes and nearly 40% particles remained in the circulation at 60 minutes; Fig. 1D). Collectively, these results indicate that PEG shielding can have a dramatic effect on the *in vitro* and *in vivo* activities of lipid nanoparticles, and optimal tumor delivery will require a properly anchored PEG shield to achieve the right balance between cellular activities and *in vivo* PK/tissue distribution properties.

Development of novel lipid nanoparticles via a 2-step screen

In view of the impact of PEG shielding on *in vitro* and *in vivo* activities, we designed a 2-step approach for the development of novel lipid nanoparticle delivery systems. In the first step, novel cationic lipids were formulated with DSPC, cholesterol, and PEG-cholesterol to form "rapid-deshielding" lipid nanoparticles for *in vitro* determination of transfection activity. Because of its short cholesterol anchor, PEG-cholesterol is expected to shed quickly from the particle under tissue culture conditions, yielding a "naked" particle for active transfection. Therefore, the PEG-cholesterol-shielded lipid nanoparticles allow us to examine the "intrinsic" ability of the cationic lipid to mediate siRNA transfection without interference from the PEG shield. An example of the *in vitro* screen is shown in Fig. 2A, where different lipids were formulated into PEG-cholesterol-shielded nanoparticles containing the tetR siRNA and tested for transfection activities in the TetR-ODC-Luc cells. Nanoparticles containing cationic lipid A-066 induced a robust increase of luciferase activity, suggesting that A-066 may be a promising component for developing novel siRNA delivery systems.

In the second step, cationic lipids that show promise from *in vitro* screen were used to form nanoparticles containing various commercial or proprietary PEG lipids. These nanoparticles were then screened *in vivo* using the positive-readout tumor models to identify the appropriate PEG shields for a particular cationic lipid. An example of the *in vivo* screen is shown in Fig. 2B. A-066 was formulated with DSPC/cholesterol, different PEG lipids, and the TetR siRNA. The resulting nanoparticles were tested for siRNA delivery using the TetR-ODC-Luc cell-derived orthotopic liver tumor model. A number of nanoparticles induced a significant increase of luminescent signal, indicating successful siRNA delivery into tumors. Among these, the A-066-derived nanoparticles containing PEG shields formed by TMH400, PEG-DPG, or PEG-DMG seemed to exhibit the best *in vivo* activity. These stepwise *in vitro* and *in vivo* screens led to the identification of a number of promising cationic lipids and PEG lipids for siRNA delivery (16).

Once a promising pair of cationic lipid and PEG lipid was identified, formulation optimization was carried out by varying the percentage of cationic lipid or PEG-lipid, using different neutral lipids, or altering formulation conditions such as processing temperature, buffer pH, etc. These formulation variants were then tested for various physiochemical properties and for *in vivo* delivery efficiency in the TetR-ODC-Luc liver tumor models to select the best candidate (17). From these studies, nanoparticles containing A-066/TMH400/DSPC/cholesterol at a 40/2/10/48 molar ratio and a total lipid/siRNA ratio of 25:1 emerged as one of the most active *in vivo* formulations that also maintain desirable properties such as excellent formulation reproducibility, uniform 100 nm particle size with PDI < 0.1, a close to neutral surface charge, and more than 6 months stability in PBS etc. (data not shown).

A-066/TMH400 exhibits similar tumor delivery efficiency as SNALP but triggers less adverse effects

Because SNALP is perceived as one of the best siRNA delivery system in the field, we compared A-066/TMH400 nanoparticles with SNALP for their abilities to deliver siRNA into tumors and their potential adverse impact on the liver, a major target tissue for lipid nanoparticles. A-066/TMH400 containing the tetR siRNA (A-066/TMH400-siTetR) produced a similar or better degree of target knockdown compared to SNALP-siTetR in the positive readout model (Fig. 3A). Intravenous administration of A-066/TMH400 containing a siRNA targeting the human Ran gene (A-066/TMH400-hRAN) also knocked down Ran to a similar extent as SNALP-hRAN in the HepG2 liver tumors (Fig. 3B). Furthermore, intravenous administration of A-066/TMH400-hRAN (2 mg siRNA/kg, i.v., twice/week for 3 weeks) produced

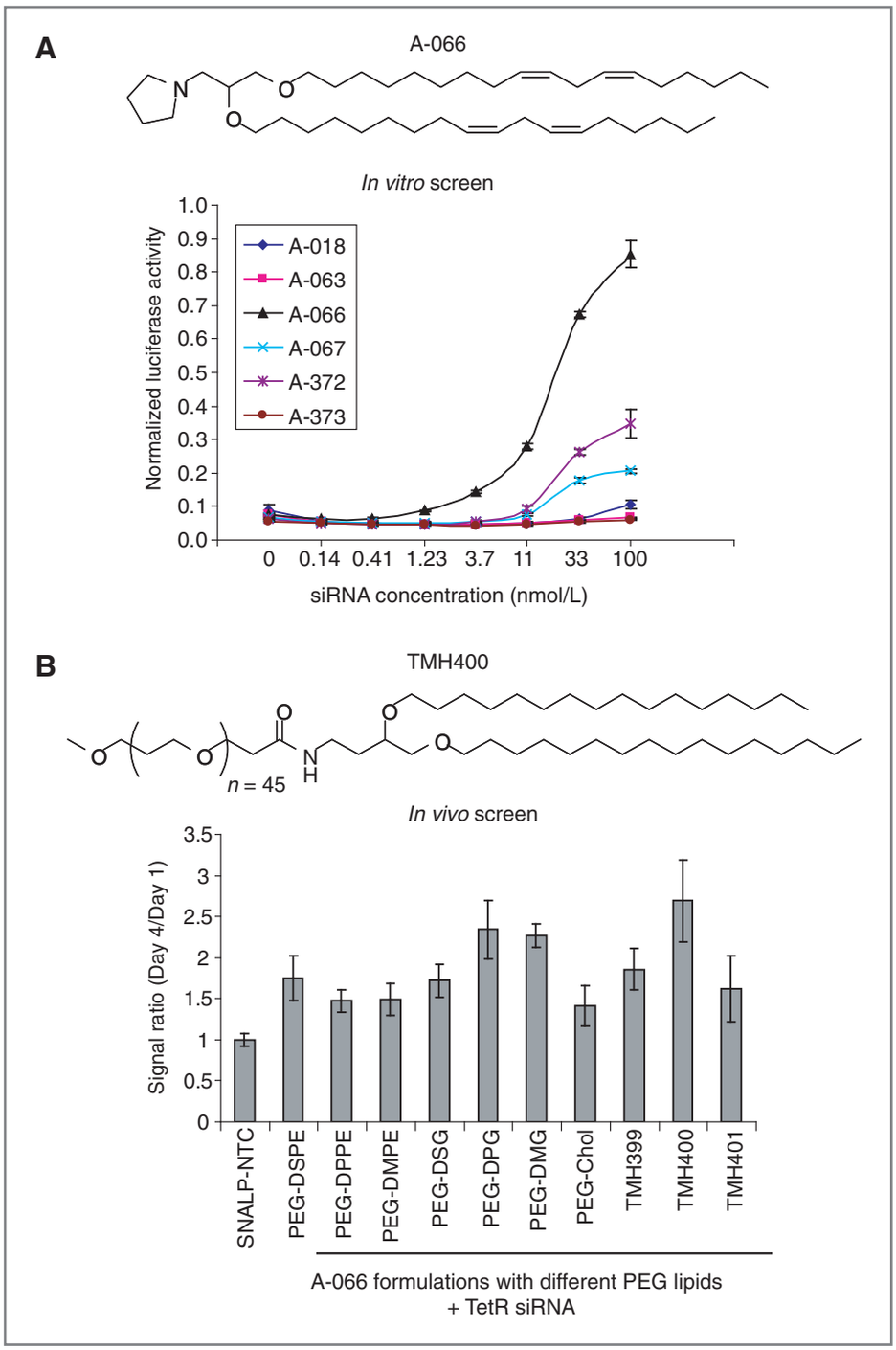

Figure 2. *In vitro* and *in vivo* screen of lipid nanoparticles. A, lipid nanoparticles were created by formulating various novel cationic lipids with DSPC, cholesterol, PEG-cholesterol, and the TetR siRNA using a 25:1 lipid/siRNA ratio and a 48/40/10/2 molar ratio of cholesterol/cationic lipids/DSPC/PEG-cholesterol. Resulting nanoparticles were incubated with the TetR-ODC-Luc cells for 72 hours, and luciferase activities were determined using the SteadyGlo Luciferase Assay kit. The resulting luciferase activities in lipid nanoparticle-treated cells were further normalized to the luciferase activity in TetR-ODC-Luc cells that were incubated with doxycycline for 3 days, and the normalized results are presented as normalized luciferase activity. B, A-066–derived lipid nanoparticles were created by formulating the TetR siRNA with A-066, DSPC, cholesterol, and various PEG-lipids using a 25:1 lipid/siRNA ratio and a 48/40/10/2 molar ratio of cholesterol/A-066/DSPC/PEG-lipids. SNALP containing a nontargeted control siRNA (SNALP-NTC) or A-066–derived lipid nanoparticles containing the TetR siRNA were administered to mice bearing the TetRODC-Luc liver tumors (i.v. 2.5 mg siRNA/kg for 2 consecutive days; $n = 5$/group). Mice were imaged before dosing (Day 1) and 48 hours after last dose (Day 4). Higher Day 4/Day 1 signal ratio indicates better knockdown of TetR in tumors after lipid nanoparticle-mediated siRNA delivery.

robust antitumor efficacy in the HepG2 liver tumor model. The degrees of tumor growth inhibition produced by A-066/TMH400-hRAN is at least equivalent, if not better, compared to what was obtained in the same model using SNALP-hRAN with the same dose and schedule in our earlier studies (23% T/C by A-066/TMH400-hRAN vs. 31% by SNALP-hRAN, comparing efficacy in Fig. 3C with efficacy in our earlier report (18).

Interestingly, although A-066/TMH400 and SNALP delivered siRNA into tumors with largely equivalent efficiency, their impact on the liver seemed to be different. In a 3-day liver toxicity study, intravenous administration of SNALP containing a control siRNA (SNALP-NTC) for 2 consecutive days induced high levels of the liver enzymes ALT and AST at doses of 5 mg/kg or higher (Fig. 4A) and caused a pronounced discoloring of

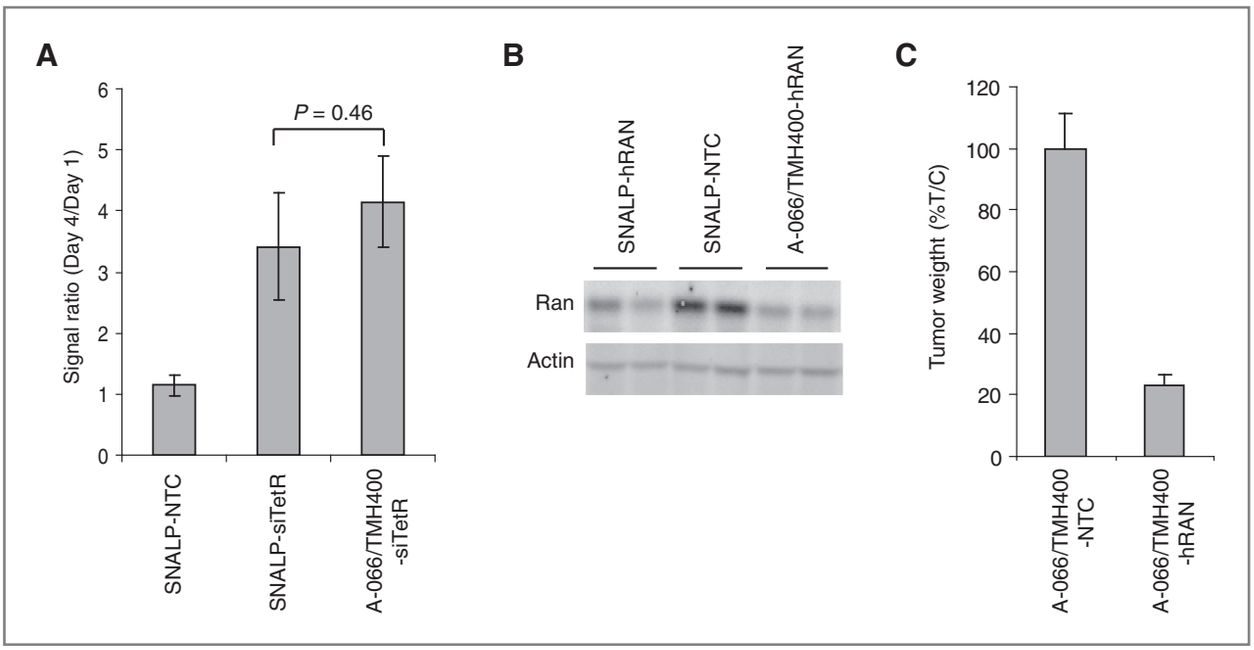

Figure 3. A-066/TMH-400 lipid nanoparticles and SNALP exhibited similar *in vivo* activity. A, the *in vivo* activities of SNALP-NTC, SNALP-siTetR, and A-066/TMH400-siTetR were determined in the TetR-ODC-Luc liver tumor model ($n = 5$/group). B, mice bearing the HepG2 liver tumors were administered (i.v. 2.5 mg siRNA/kg for 3 days) SNALP-NTC or SNALP and A-066/TMH400 lipid nanoparticles containing a siRNA that specifically targets the human but not mouse Ran gene (SNALP-hRAN and A-066/TMH400-hRAN). Tumor tissues were collected and the amounts of the RAN protein in each sample were determined by Western analysis. Each lane represents a sample from individual mouse. C, mice bearing the HepG2 liver tumors were administered (i.v. 2.5 mg siRNA/kg, twice/week for 3 weeks) A-066/TMH400 lipid nanoparticles containing a control siRNA (A-066/TMH400-NTC) or the Ran siRNA (A-066/TMH400-hRAN). Tumor weights at the end of the study were determined and the average tumor weight and standard error are presented ($n = 10$/group).

the liver (data not shown), indicating that SNALP caused liver damage at these doses. In contrast, neither significant induction of liver enzymes nor liver color change was observed for A-066/TMH400-NTC at all doses, suggesting that the A-066/TMH400 nanoparticles are better tolerated (Fig. 4A, right). To understand the different tolerability between SNALP and A-066/TMH400, we produced SNALP and A-066/TMH400 lipid nanoparticles containing an Alexa647-labled siRNA so that fluorescent siRNA signals can be quantified as an indirect measurement of the amount of nanoparticles in circulation and in the liver. Higher concentrations of the fluorescent siRNA was detected in A-066/TMH400-treated mice versus SNALP treated mice at both 8 and 24 hours after intravenous injection of A-066/TMH or SNALP containing the Alexa647-labled TetR siRNA at 5 mg siRNA/kg, indicating that A-066/TMH400 stayed in circulation longer than SNALP. In addition, less amounts of the fluorescent siRNA were detected in the liver of A-066/TMH400-treated mice versus SNALP-treated mice, suggesting that A-066/TMH400 may accumulate less in the liver than SNALP, which could partially explain the better tolerability A-066/TMH400 compared to SNALP (Fig. 4B, left panel and Fig. 4C). Interestingly, the differences in circulating time and liver accumulation between A-066/TMH400 and SNALP became more pronounced in rats, suggesting that A-066/TMH400 and SNALP may potentially have greater tolerability differences in larger animals (Fig. 4B, right panel and Fig. 4C).

Selection of therapeutic targets and siRNA molecules

Although lipid nanoparticles are by far the most efficient siRNA delivery system in our hands, they are far from ideal in their tumor delivery efficiency. For example, we have shown previously that SNALP-like lipid nanoparticles only deliver siRNAs to areas adjacent to tumor blood vessel, and consequently, high degrees of tumor vascularization is often required for efficient siRNA delivery (18). In fact, when SNALP was used for siRNA delivery, even in the highly vascularized HepG2 liver tumors, significant target knockdown was only observed using a hyper-potent Ran siRNA ($EC_{50} = 0.09$ nmol/L) but not a fairly potent Bcl-XL siRNA ($IC_{50} = 0.9$ nmol/L). In contrast, robust target knockdown in the liver was observed using the same Bcl-XL siRNA, suggesting that SNALP delivers siRNA more efficiently into liver than tumor (data not shown). Taken all together, we believe that with the limitations of current delivery systems, significant therapeutic benefit will most likely be obtained in highly vascularized tumors (e.g., HCCs) using an exceptionally potent siRNA against a very robust therapeutic target. In addition, the therapeutic siRNA should be highly selective

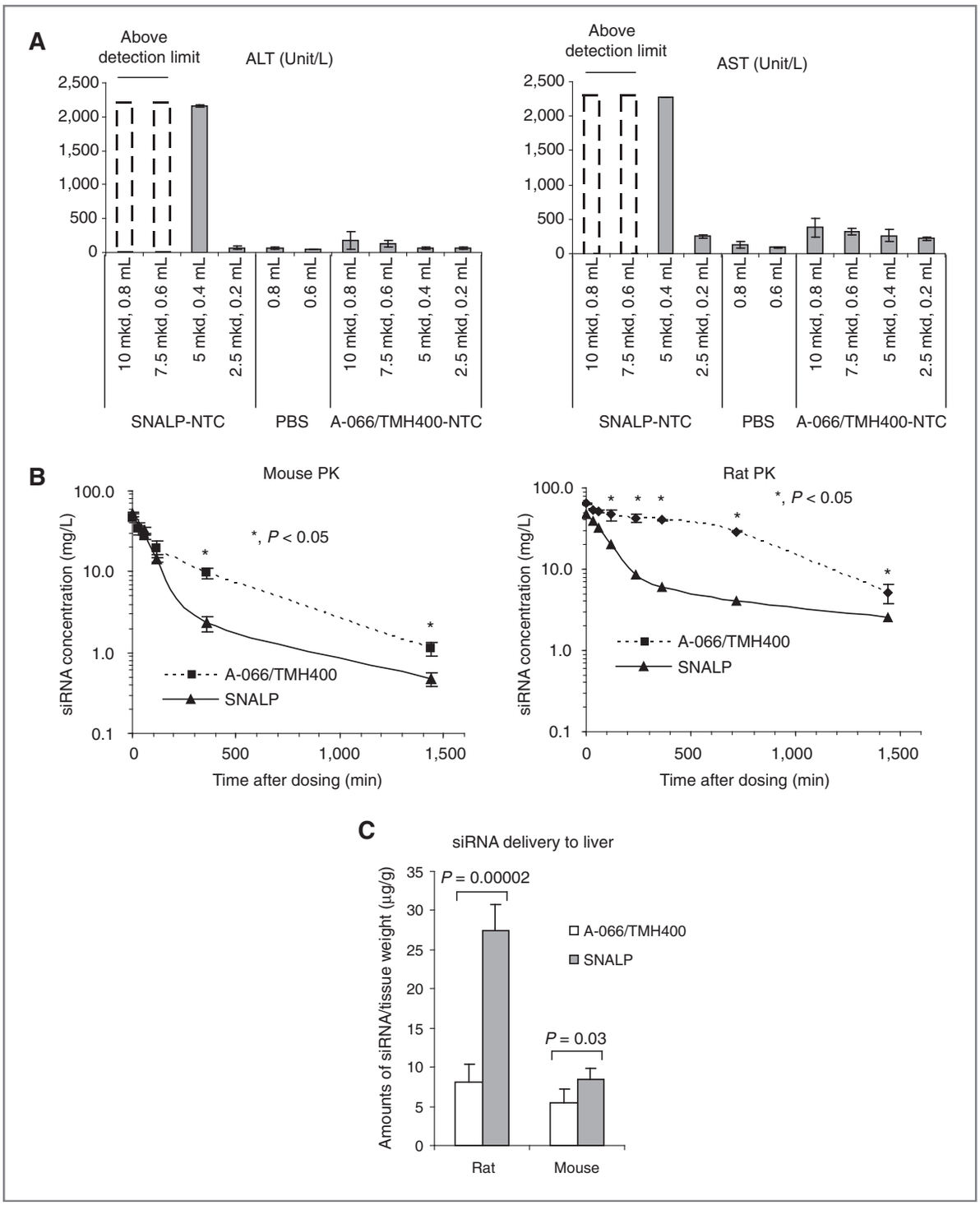

Figure 4. A-066/TMH400 lipid nanoparticles exhibited better tolerability compared to SNALP. A, nontumor-bearing *SCID* female mice were administered PBS or SNALP and A-066/TMH400 lipid nanoparticles containing the control siRNA (SNALP-NTC and A-066/TMH400-NTC) for 2 consecutive days using the indicated amounts and volume. Serum ALT (left) and AST (right) levels were determined afterward. B, A-066/TMH400 and SNALP lipid nanoparticles containing an Alexa647-labled TetR siRNA were administered to each animal (i.v. 5 mg siRNA/kg). Plasma samples were collected at indicated time ($n = 3$/time point for mice, and $n = 3$ via serial bleeding for rat). The Alexa647 signal was then quantified using the IVIS 200 luminescence imaging system, and siRNA concentrations in circulation were determined using a standard curve of Alexa647-labled TetR siRNA diluted in mouse or rat plasma. *P* values were obtained for each time point using paired 2 tail *t* test. *, $P < 0.05$. C, animals from B were sacrificed at the end of the study to collect liver tissues. The Alexa647 signal in liver was quantified using the IVIS 200 system after the livers were weighed and homogenized. siRNA concentrations in the liver were determined using a standard curve of Alexa647-labled TetR siRNA spiked in the mouse or rat liver homogenates. *P* values were obtained using paired 2 tail *t* test.

in killing tumor cells relative to liver cells to avoid the toxicity associated with target inhibition in the liver.

The *in vivo* efficacy/toxicity profile of a therapeutic siRNA ultimately reflects the combination of 3 interconnected factors that include: (i) potency of the best available siRNA, (ii) the biological robustness of the underlying targets for cancer cells, and (iii) the selectivity for cancer over liver cells. Thus, we used an empirical approach that takes these 3 factors into consideration for the selection of therapeutic targets and siRNA molecules. This approach encompasses the following steps: (i) identify potent cross species siRNA (human/mouse) against chosen targets; (ii) determine the *in vivo* tolerability of siRNA-containing lipid nanoparticles (2.5 mg siRNA/kg, i.v. twice/week for 3 weeks) to eliminate targets that cause liver damage or other tolerability issues when knocked down; (iii) for siRNA-containing lipid nanoparticles that are well tolerated, assess the anti-tumor efficacy in an orthotopic liver tumor model to identify efficacious target and siRNA molecules; and (iv) confirm that the observed antitumor efficacy does not result from immune stimulation by examining the ability of each lipid nanoparticle to trigger siRNA-mediated immune response. An example of our target selection process is shown in Table 1 and Fig. 5. In this example, 13 candidate targets were first selected based on literature reports or internal siRNA library screening results. *In silico* siRNA sequence selection was then carried out using a proprietary siRNA scoring algorithm, and the top 50 algorithm-selected siRNAs for each target were transfected into HeLa cells at different concentrations to determine their abilities to induce target knockdown at the mRNA level. Contrary to the conventional wisdom that potent siRNAs can be easily identified for a given target, we failed to obtain any siRNAs that meet our potency criteria ($IC_{50} < 1$ nmol/L) for either the human or mouse homologues of Aurora B, KNTC, and

Table 1. Best siRNA sequences and *in vivo* tolerability of candidate targets

				Targeting species		Tolerability assessment	
siRNA	Target	siRNA sequence (sense strand, overhang not shown)	IC_{50} (nmol/L) (siSTABLE)	Human	Mouse	Body weight change	Liver toxicity
NTC	N/A	UGGUUUACAUGUUGUGUGA	N/A	N/A	N/A	4%	No
hRAN_1.21	Ran	GUGUGCCACCUCAUUAUUA	0.07	X	No	7%	No
KRAS_1.24	KRAS	UGCAGUUGAUUACUUCUUA	0.04	X	No	4%	No
KRAS_1.17	KRAS	GCAUGCAGUUGAUUACUUC	0.08	X	No	5%	No
BIRC5_1.10	BIRC5	GAGACAGAAUAGAGUGAUA	0.15	X	No	6%	No
BIRC5_1.14	BIRC5	GUAGAUGCAUGACUUGUGU	0.11	X	No	6%	No
NHP2L1_1.1	NHP2L1	GCUGUGUGAAGACAAGAAU	0.16	X	X	2%	No
NHP2L1_1.6	NHP2L1	GCUGCUGUGUGAAGACAAG	0.12	X	X	3%	No
CDCA1_1.2	CDCA1	GUGGCAUUAUCAACUUUAU	0.25	X	X	8%	No
CDCA1_1.5	CDCA2	CAACUUUAUUCACUUCAGA	0.67	X	X	5%	No
EIF3S6_1.14	EIF3S6	UCUUAAUGCAGAAUUGGGA	0.002	X	X	4%	No
EIF3S6_1.18	EIF3S6	CAGCCAUGGAAGACCUUAC	0.003	X	X	0%	No
RPL37A_1.12	RPL37A	GGUGAAGAAAAUUGAAAUC	0.026	X	X	−32%	Yes
RPL37A_1.1	RPL37A	CCGGAAAAUGGUGAAGAAA	0.044	X	X	−14%	Yes
RPS21_1.6	RPS21	UGAACGUGGCCGAGGUUGA	0.02	X	X	−10%	Yes
RPS21_1.9	RPS21	GCGAGUUCGUGGACCUGUA	0.007	X	X	0%	Yes
PSMA2_1.7	PSMA2	CGACCAUAUUUAUUUCAGU	0.015	X	X	−10%	Yes
PSMA2_1.17	PSMA2	AUCUUAACCCUAAAGGAAA	0.014	X	X	−11%	Yes
PSMD2_1.10	PSMD2	AGACUGAGCUCAAGGAUAC	0.0002	X	X	−13%	Yes
PSMD2_1.17	PSMD2	GAAGGAAAUCUAUGAGAAC	0.0001	X	X	−25%	Yes
RAN_1.1	RAN	AGAAGAAUCUUCAGUACUA	0.09	X	X	Death after 2 doses	Yes
RAN_1.6	RAN	GCAUAGAGAUCUGGUACGA	0.06	X	X	Death after 2 doses	Yes
KIF11_1.1	KIF11_1.1	GAGAAGAGCUUGUUAAAAU	1.47	X	X		
Aurora B	Aurora B	IC50 > 5 nM for all siRNAs					
KNTC	KNTC	IC50 > 5 nM for all siRNAs					

NOTE: To determine the IC_{50} of siRNA, each siRNA was transfected into relevant cancer cell lines using Lipofectamine 2000. mRNA level of the target gene was then determined using the branched DNA assay. For tolerability determination, each siRNA was formulated into the lipid nanoparticle formulation and administered via i.v. into nontumor-bearing mice at 2 mg siRNA/kg, twice/week for 3 weeks. Tolerability was monitored via body weight change, increase of ALT and AST, as well as gross liver morphology and color changes at the end of the dosing period.

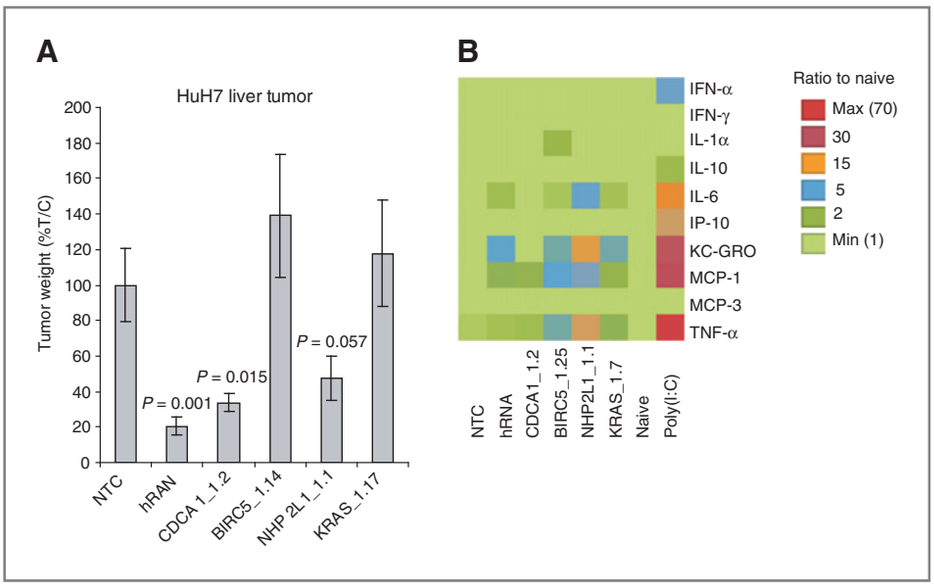

Figure 5. Selection of therapeutic targets and siRNA molecules. A, A-066/TMH400 lipid nanoparticles containing indicated siRNAs were administered to mice bearing the HuH7 liver tumors (i.v. 2.5 mg siRNA/kg, twice/week, for 3 weeks). Liver tumors were collected and tumor weights were determined. *Y*-axis represents the average tumor weight and standard error in each treatment group ($n = 10$/group). *P* values were obtained by comparing the indicated treatment group with the NTC group using paired 2 tail *t* test. B, *SCID* females were either untreated (Naïve), treated with poly (I:C), or administered A-066/TMH400 lipid nanoparticles containing indicated siRNAs. Serum samples were collected 2 hours after dosing and the levels of 10 cytokines and chemokines were determined using an Luminex-based multiplex assay. Different colors indicate the ratio of the amounts of each analyte in treated versus untreated naïve animals.

KIF11. Considering that target knockdown in tumors will likely require very potent siRNAs as indicated by the failure of the Bcl-XL siRNA ($IC_{50} = 0.9$ nmol/L) to knockdown its target in the HepG2 liver tumors, the low potency siRNAs against Aurora B, KNTC, and KIF11 are not suitable for further evaluation of potential antitumor efficacy produced by inhibiting these targets. Although highly potent siRNAs targeting human K-Ras and BIRC5 genes were obtained, we failed to identify siRNAs targeting their mouse homologues with our desired potency, thus preventing us from evaluating the potential toxicity associated with inhibiting these targets. For the 8 targets that have potent, cross species siRNAs available, lipid nanoparticles containing siRNAs against RPL37A, PRS21, PSMA2, PSMD2, and RAN (2 siRNAs/target) caused severe toxicity as judged by liver color change, significant elevation of ALT, AST, and significant body weight loss. Although lipid nanoparticles containing the EIF3S6 siRNA (EIF3S6_1.14) did not trigger any obvious adverse effects in the tolerability screen in healthy mice, the same particles caused multiple deaths in mice carrying the orthotopic HuH7 liver tumors during efficacy trials (data not shown). We suspect that the HuH7 liver tumor burden may exacerbate the adverse effect of knocking down EIF3S6 in the liver, resulting in a reduction of tolerability in tumor-bearing mice. Collectively, these results further highlight the needs of identifying therapeutic targets that, upon knockdown, do not adversely affect liver function. Among siRNAs that are well tolerated, lipid nanoparticles containing the siRNA-targeting CDCA1 (CDCA1_1.2) significantly inhibited the growth of the orthotopic HuH7 liver tumor, and lipid nanoparticles containing the siRNA-targeting NHP2L1 (NHP2L1_1.1) also exhibited moderate tumor growth inhibition. In contrast, no antitumor efficacy was observed for siRNAs targeting KRAS and BIRC5 (Fig. 5A). A testing of cytokines/chemokines in mice treated with various lipid nanoparticles revealed that the lipid nanoparticles containing NHP2L1_1.1 caused a moderate increase of several cytokines/chemokines, making it difficult to distinguish whether the observed antitumor efficacy is truly target related or resulted from siRNA-mediated immune stimulation. In contrast, no significant cytokine/chemokine induction was observed using lipid nanoparticles containing CDCA1_1.2, indicating that the antitumor efficacy produced by A-066/TMH400-CDCA1_1.2 is unlikely because of siRNA-mediated immune response (Fig. 5B). Accordingly, A-066/TMH400-CDCA1_1.2 represents a promising starting point for the development of siRNA-based therapy for HCC.

Discussion

The lack of clinically relevant methods for delivering siRNA into tumors remains a major technical hurdle for the development of therapeutic siRNA for oncology indications. To deliver siRNA into tumors via the systemic route, the delivery system need to satisfy the following requirements: (i) protects siRNA from nuclease degradation in circulation, (ii) exhibits a proper PK and tissue distribution profile to deliver siRNA to disease-relevant

organs/tissues, and (iii) facilitates efficient uptake of siRNA into target cells and releases siRNA into cytoplasma to knockdown the target. Technical solutions for each individual requirement largely exist owning to several decades of research on gene delivery technologies. However, to integrate all solutions into one delivery system is highly challenging. In particular, properties that are beneficial for cellular activities such as highly positive surface charge and high fusogenicity are often detrimental for PK properties that are critical for *in vivo* performance. Conversely, attempts to stabilize/shield nanoparticles in the bloodstream to improve the PK and tissue distribution profile often reduce the ability of nanoparticles to enter cells or escape from endosome, leading to a reduction or loss of cellular activity. Some of these issues were exemplified by the differential *in vitro* and *in vivo* activities of lipid nanoparticles with various PEG shields. As shown in Fig. 1, nanoparticles with the optimal *in vitro* activity did not exhibit any meaningful activity *in vivo* likely due to their poor PK properties whereas particles without *in vitro* activity turn out to be highly active *in vivo*.

It has been shown that the strength of the interaction between the anchor moiety on PEG and the membrane lipids determines the rate and extent of PEG-lipid extraction/exchanging to plasma proteins. PEG-lipids with longer acyl chain confer stronger interaction with membrane lipids thus less likely to be extracted/exchanged, and consequently, PEGs with longer lipid anchor are often associated with a slower rate of deshielding (15, 19–21). Our results suggest that PEG-DMPE may be shed rapidly to expose the "naked" lipid particle consisting of fusogenic lipid D-Lin-DMA, which allows it to fuse with the cell membrane to achieve efficient siRNA transfection *in vitro*. However, rapid deshielding of PEG-DMPE may led to a fast clearance of lipid nanoparticles *in vivo*, which likely prevents it from reaching tumors in sufficient quantify and causes suboptimal *in vivo* delivery. By contrast, lipid nanoparticle containing PEGs with longer lipid anchors (PEG-DPPE and PEG-DSPE) may deshield slowly, causing diminished *in vitro* activity. However, these well-shielded nanoparticles stay in the circulation longer and thus have better chance to reach the tumor site via the enhanced permeability and retention effect. These lipid nanoparticles eventually deshield inside tumors and result in successful *in vivo* delivery. These results suggest that a successful delivery system needs to strike an exquisite balance between the cellular activity and the *in vivo* PK/tissue distribution properties to obtain optimal delivery efficiency *in vivo*. To find the right balance, changes made on the delivery system need to be tested *in vivo* to determine whether the alteration is beneficial or detrimental. The previously described positive-readout tumor model provides a convenient tool for relatively rapid *in vivo* screening of delivery formulations. Using this model, we screened hundreds of lipid nanoparticles for tumor delivery and identified A-066/TMH400 as a promising delivery system for the development of a siRNA therapy for cancer treatment. It is noteworthy that TMH400 and A-066 are structurally similar to PEG-C-DMA and D-lin-DEA, a close analog of D-lin-DMA. Nonetheless, the final lipid nanoparticles made of A-066/TMH400 exhibited a significantly different toxicity profile compared to SNALP, indicating that small changes on lipid structure could potentially result in unexpected significant differences in the nanoparticles.

Lipid nanoparticles delivered siRNA into tumors more efficiently than many other delivery systems reported in the literature, but still have their limitations such as the preferential delivery to liver versus tumor and the inability to deliver siRNA to areas farther away from tumor vasculature. With these limitations, proper selection of disease indications, disease targets, and the best siRNA molecule against a chosen target becomes imperative to circumvent deficiencies associated with an imperfect delivery platform. In this study, we examined a set of targets for the availability of hyper potent siRNAs, potential toxicities resulted from target knockdown, and the antitumor efficacy of inhibiting these targets in an orthotopic liver tumor model. From these analyses, CDCA1 emerged as a promising target for the development of siRNA-based therapy for HCC. CDCA1 is part of the kinetochore-associated NDC80 complex, which is essential for chromosome segregation and spindle checkpoint function. siRNA-mediated targeting of CDCA1 potentially represents a new way of disrupting the mitotic machinery for cancer therapy. The emphasis on using an extremely potent siRNA for the development of siRNA therapy is often overlooked. It is important to recognize that improving the best currently available delivery system to achieve a 10-fold better delivery efficiency will be extremely difficult. However, obtaining a 10- to 100-fold more potent siRNA for a given target or finding a biologically equivalent target for which there is a 10- or 100-fold more potent siRNA available are technically feasible and may achieve the same or better therapeutic effect than a 10-fold improvement on the delivery system. Toward this end, the efficacy/toxicity profile of the A-066/TMH400-CDCA1_1.2 formulation can be greatly improved if a more potent CDCA1 siRNA can be obtained via a thorough siRNA sequence search or by incorporating chemical modifications to boost siRNA potency. It is noteworthy that the potency of the best siRNA differs significantly across targets (ranging from 0.001 to >5 nmol/L), which may result from the intrinsic differences on target sequence and/or the secondary structure of target mRNA. Therefore, it is conceivable that carrying out an extensive siRNA sequence search on CDCA1 partners within the NDC80 complex may reveal siRNAs that trigger the same biological response as the CDCA1_1.2 siRNA but with significantly better potency than the current CDCA1 siRNA, which could be a promising alternative toward obtaining better therapeutic formulations than the current A-066/TMH400_CDCA1_1.2 lipid nanoprticles.

Disclosure of Potential Conflicts of Interest

No potential conflicts of interest were disclosed.

Authors' Contributions

Conception and design: L. Li, R. Wang, A. Sarthy, L. Tian, P. Dande, R.D. Hubbard, T.M. Hansen, C. Wada, X. Zhao, S.W. Fesik, Y. Shen
Development of methodology: L. Li, R. Wang, A. Sarthy, X. Lin, X. Huang, L. Tian, P. Dande, X. Zhao, Y. Shen
Acquisition of data (provided animals, acquired and managed patients, provided facilities, etc.): L. Li, R. Wang, D. Wilcox, A. Sarthy, P. Dande, X. Zhao
Analysis and interpretation of data (e.g., statistical analysis, biostatistics, computational analysis): L. Li, R. Wang, D. Wilcox, A. Sarthy, X. Huang, L. Tian, P. Dande, X. Zhao, W.M. Kohlbrenner, Y. Shen
Writing, review, and/or revision of the manuscript: L. Li, R. Wang, A. Sarthy, X. Lin, C. Wada, X. Zhao, W.M. Kohlbrenner, Y. Shen
Administrative, technical, or material support (i.e., reporting or organizing data, constructing databases): R. Wang, Y. Shen
Study supervision: L. Li, W.M. Kohlbrenner, S.W. Fesik, Y. Shen

Grant Support

This work was supported by Abbott Laboratories' internal R&D fund.

The costs of publication of this article were defrayed in part by the payment of page charges. This article must therefore be hereby marked *advertisement* in accordance with 18 U.S.C. Section 1734 solely to indicate this fact.

Received October 15, 2012; revised June 28, 2013; accepted July 29, 2013; published OnlineFirst August 13, 2013.

References

1. de Fougerolles A, Vornlocher HP, Maraganore J, Lieberman J. Interfering with disease: a progress report on siRNA-based therapeutics. Nat Rev Drug Discov 2007;6:443–53.
2. Shen Y. Advances in the development of siRNA-based therapeutics for cancer. IDrugs 2008;11:572–8.
3. Li L, Shen Y. Overcoming obstacles to develop effective and safe siRNA therapeutics. Expert Opin Biol Ther 2009;9:609–19.
4. Akinc A, Zumbuehl A, Goldberg M, Leshchiner ES, Busini V, Hossain N, et al. A combinatorial library of lipid-like materials for delivery of RNAi therapeutics. Nat Biotechnol 2008;26:561–9.
5. Aleku M, Schulz P, Keil O, Santel A, Schaeper U, Dieckhoff B, et al. Atu027, a liposomal small interfering RNA formulation targeting protein kinase N3, inhibits cancer progression. Cancer Res 2008;68:9788–98.
6. Hu-Lieskovan S, Heidel JD, Bartlett DW, Davis ME, Triche TJ. Sequence-specific knockdown of EWS-FLI1 by targeted, nonviral delivery of small interfering RNA inhibits tumor growth in a murine model of metastatic Ewing's sarcoma. Cancer Res 2005;65:8984–92.
7. Zimmermann TS, Lee AC, Akinc A, Bramlage B, Bumcrot D, Fedoruk MN, et al. RNAi-mediated gene silencing in non-human primates. Nature 2006;441:111–4.
8. Rozema DB, Lewis DL, Wakefield DH, Wong SC, Klein JJ, Roesch PL, et al. Dynamic polyconjugates for targeted in vivo delivery of siRNA to hepatocytes. Proc Natl Acad Sci U S A 2007;104:12982–7.
9. Judge AD, Robbins M, Tavakoli I, Levi J, Hu L, Fronda A, et al. Confirming the RNAi-mediated mechanism of action of siRNA-based cancer therapeutics in mice. J Clin Invest 2009;119:661–73.
10. Semple SC, Akinc A, Chen J, Sandhu AP, Mui BL, Cho CK, et al. Rational design of cationic lipids for siRNA delivery. Nat Biotechnol 2010;28:172–6.
11. Lin X, Li L, Wang R, Wilcox D, Zhao X, Song J, et al. A robust *in vivo* positive-readout system for monitoring siRNA delivery to xenograft tumors. Rna 2011;17:603–12.
12. Wheeler JJ, Palmer L, Ossanlou M, MacLachlan I, Graham RW, Zhang YP, et al. Stabilized plasmid-lipid particles: construction and characterization. Gene Ther 1999;6:271–81.
13. Morrissey DV, Blanchard K, Shaw L, Jensen K, Lockridge JA, Dickinson B, et al. Activity of stabilized short interfering RNA in a mouse model of hepatitis B virus replication. Hepatology (Baltimore, MD) 2005;41:1349–56.
14. Heyes J, Palmer L, Bremner K, MacLachlan I. Cationic lipid saturation influences intracellular delivery of encapsulated nucleic acids. J Control Release 2005;107:276–87.
15. Judge A, McClintock K, Phelps JR, Maclachlan I. Hypersensitivity and loss of disease site targeting caused by antibody responses to PEGylated liposomes. Mol Ther 2006;13:328–37.
16. Dande PA, Hansen TM, Hubbard RD, Sarthy AV, Shen Y, Tian L, et al., inventors; Abbott Laboratories, assignee. Cationic lipids and uses thereof. United States patent US 20100104629. 2010 Apr 29.
17. Zhao X, Liu Y, Song J, Yong H, Li L, Shen Y, et al. Cationic lipids percentage and processing temperature are critical in designing siRNA lipid nanoparticles. J Drug Target 2012;20:281–9.
18. Li L, Wang R, Wilcox D, Zhao X, Song J, Lin X, et al. Tumor vasculature is a key determinant for the efficiency of nanoparticle-mediated siRNA delivery. Gene Ther 2012;19:775–80.
19. Li WM, Xue L, Mayer LD, Bally MB. Intermembrane transfer of polyethylene glycol-modified phosphatidylethanolamine as a means to reveal surface-associated binding ligands on liposomes. Biochim Biophys Acta 2001;1513:193–206.
20. MacLachlan I, Cullis P. "Diffusible-PEG-lipid stabilized plasmid lipid particles." Adv Genet 2005;53:157–88.
21. Silvius JR, Zuckermann MJ. Interbilayer transfer of phospholipid-anchored macromolecules via monomer diffusion. Biochemistry 1993;32:3153–61.